



ACOUSTICS 2012

Simulations on Active Fan Noise Control

H. Fischer

EADS Deutschland GmbH, EADS Innovation Works Germany, 81663 München, Germany
helen.fischer@eads.net

Noise reduction by active noise control (ANC) in jet engines and its prediction is of high interest, since the acoustic goals of flightpath 2050 can hardly be achieved by passive acoustic treatments. Numerous former test campaigns showed that significant noise reduction is possible by active noise control. Simulations are needed for further understanding of test results and in order to predict the noise reduction and possibly impact on the performance of future jet engines. Therefore an ANC prediction tool in frequency domain based on a common 3D CAA solver has been developed. The tool is validated by measurements in a simple straight duct with wall mounted sensors and loudspeakers. The primary sound field has one dominant azimuthal mode order. Varying complexity of the control concept leads to significant distinct results in noise reduction and the input signals of control sources. Later application of the tool will be the simulation of jet engines (i.e. inlet, fan, stator and nozzle). The CAA solver does not include the rotation of fan. Established models of fan scattering and sound transmission need to be implemented. The effect of the fan models on the noise control can be assumed by means of the investigated control concepts.

1 Introduction

Growing air traffic can be achieved only by the reduction of running costs. For politically reasons parts of these costs, like landing fees, are more and more related to emissions. At takeoff and landing one of the main noise sources at airplanes is the rotor stator interaction of the fan. In the early 60's Tyler and Sofrin pointed out that the interaction noise is harmonic and excites a special azimuthal mode order as a function of blade and vane number [1]. These harmonics, multiples of the blade passage frequency (BPF), shown in Figure 1 are about 30 dB louder than broad band noise. ANC of fan noise reduce the sound pressure level of these harmonics.

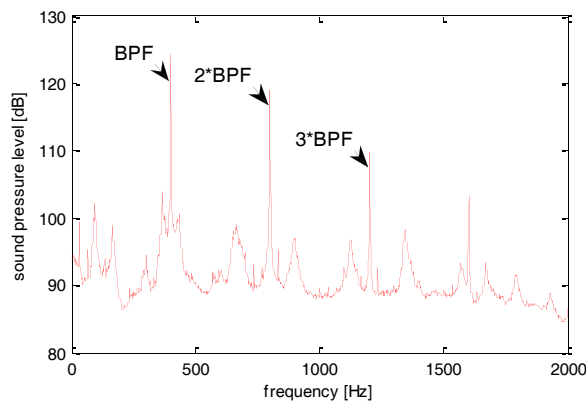


Figure 1: Measured sound pressure spectrum of rotor stator interaction noise

Simulation has become one of the basements of aircraft design and development. The main benefits are that results can be obtained cheap and fast compared with test campaigns and the variety of setup is almost infinite. For future application of ANC it is mandatory to estimate the achievable noise reduction in preliminary design phase and to reduce penalties in the performance of the engine.

The primary sound field excited by the fan interaction needs to be provided for the tool. One possibility is to use the results of a CFD calculation and extract the acoustic pressure. The active noise control system identifies the particular phase and amplitude of secondary loudspeakers to destructively superpose parts of the primary sound field by using the linearity of the system. Detailed discussion on the destructively interference of plane waves in infinite ducts can be found in Nelson&Elliot [2].

This principle also works for multiple sources and modes with higher order. One example is pictured in Figure 2, where the primary sound field of ten monopoles is

extinguished at the position of the microphones by ten nearby secondary sound sources.

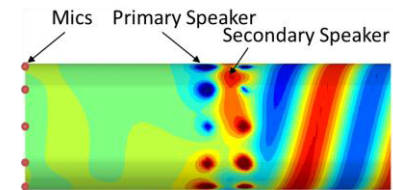


Figure 2: ANC of azimuthal mode $m=1$ in a straight duct (3D)

For the ANC simulations a common 3D CAA solver is being used in frequency domain. This solver cannot handle rotating parts as the fan. The simulation model does not contain the rotating blades. The influence of the rotor is integrated in the ANC simulation as additional transfer function which models the acoustical behavior. The modal error at the microphones e_M can get evaluated in frequency domain by the product of modal transfer function T_M and the modal excitement y_M .

$$\vec{e}_M = T_M \cdot \vec{y}_M \quad (1)$$

In equation (1) the transfer function has to include the acoustics of the duct with all vanes or struts and of the rotor. The rotor part can be excluded like shown in equation (2).

$$\begin{aligned} \vec{e}_{M_duct} &= T_{M_duct} \cdot \vec{y}_M \\ \vec{e}_M &= T_{M_rotor} \cdot \vec{e}_{M_duct} \end{aligned} \quad (2)$$

The transfer function of the parts at rest T_{M_duct} is simulated and T_{M_rotor} will be provided from transition models through the rotor.

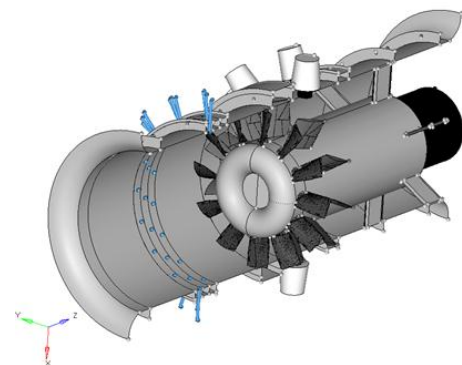


Figure 3: ROSTI fan test rig

Tests have been made with a Rotor Stator Interaction test rig (ROSTI) shown in Figure 3 to determine the transmission of acoustic modes through the fan stage. In the ANC simulation model the acoustic behavior of the fan is taken into account by transfer function and will not be modeled in the 3D model.

2 Test setup

The flow direction of the fan setup in Figure 4 is from left to right. The side view of the test rig shows the positions of the 16 loudspeakers (white) just downstream of the stator. Upstream of the stator 48 wall mounted microphones are distributed in three rings. Speakers and microphones are equally spaced in circumferential order.

The diameter of the duct is approx. 500mm.

Eight of the loudspeakers next to the stator are used to excite acoustic modes for transition tests. For control purpose all 16 speakers are needed.

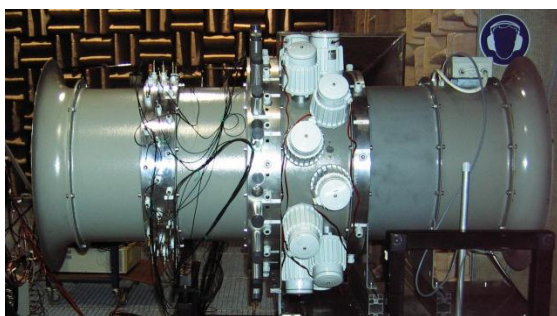


Figure 4: Side view of rotor stator interaction test rig

The stator consists of 11 vanes and the rotor has 12 blades. Figure 5 shows the distance between the rotor and the microphone rings in front of it, which is about 200mm.



Figure 5: Intake of test rig

The transmission of cut-on modes is measured with different rotational speeds.

3 Measurement results

3.1 Without rotor

The transmission matrix of acoustic modes without rotor include mode coupling of the azimuthal mode orders $m = \pm 1$ as shown in Figure 6. When exciting the azimuthal mode order $m = 1$ with the loudspeakers just downstream of the stator the microphones detect mode order $m = 1$ as well as $m = -1$ with a bit less amplitude.

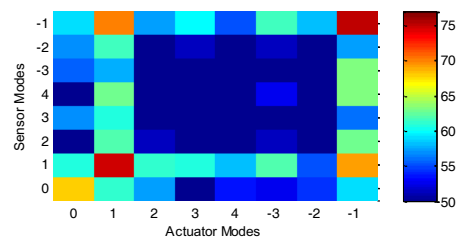


Figure 6: Amplitudes of modal transmission matrix in dB without rotor

When mode order $m = -1$ is excited, at the position of the microphones are both azimuthal mode orders $m = \pm 1$ present. This reflection is generated in the stator plane to meet the boundary condition at the stator vanes.

3.2 Rotor at rest

The influence of relative position between rotor and stator is evaluated. 13 measurements with different angles between the stator vanes and the rotor blades have been performed. The angle between two adjacent vanes is $\varphi_{stator} = 2\pi/11$ and for the rotor $\varphi_{rotor} = 2\pi/12$ (see Figure 7).

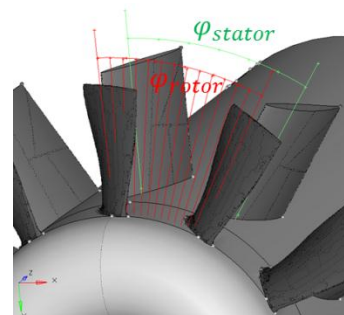


Figure 7: Angles of vanes and blades

The rotor has been turned stepwise with $\Delta\varphi_{rotor} = \frac{2\pi}{12}/13$ (red lines in Figure 7). The result of direct frequency response for the cut-on modes with different relative rotor angles is depicted in Figure 8.

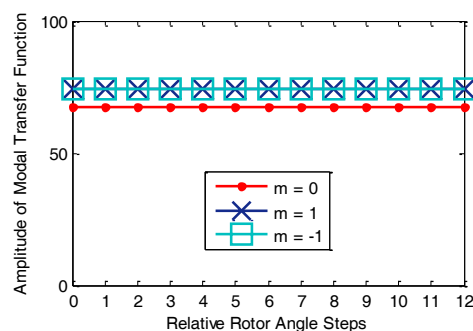


Figure 8: Amplitude of transfer function in dB with rotor at rest at 400Hz for different relative rotor angles

The modal transmission matrix in Figure 9 indicates that the presence of rotor prevent the modes coupling for the orders $m = \pm 1$.

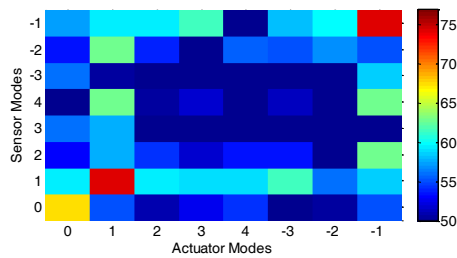


Figure 9: Amplitudes of modal transmission matrix in dB with rotor

The comparison of both set ups (with/wo rotor) in Figure 10 illustrates that the rotor at rest is an obstacle for propagating modes. As a consequence of this, the cut-on modes $m = \pm 1$ in the microphone plane are not as intense as without rotor.

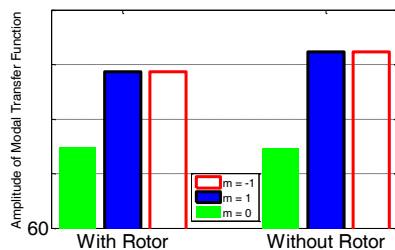


Figure 10: Comparison of modal amplitudes of transfer function in dB

The deviation in modal amplitudes equates to the reflected part of the sound field. The amplitudes of azimuthal mode $m = 0$ does not vary. The rotor has no influence on non-rotating modes. The modes $m = \pm 1$ are spinning in diverse directions and have the same amplitude in the single set-ups. The stagger angle of the rotor does not lead to an unsymmetrical behavior.

3.3 Spinning rotor

The rotation of the fan does not produce obvious additional effects to modal transfer function as diagrammed in the transmission matrix in Figure 11. No extra mode coupling compared to Figure 9 occurs.

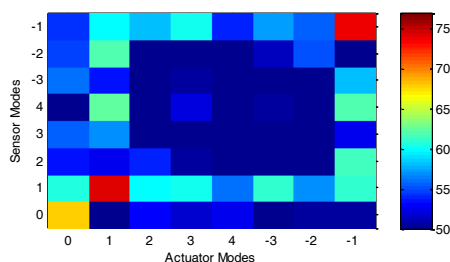


Figure 11: Amplitudes of modal transmission matrix in dB with revolving rotor at 1900 rpm

For detailed information about the influence of the circling rotor spinning modes with the orders $m = \pm 1$ for $f = 420\text{Hz}$ are excited separately by the loudspeakers and measured in the microphone plane. While with rotor at rest these amplitudes are equal (see Figure 8) does Figure 12 demonstrate big divergence in modal amplitudes between these modes. The mode $m = 1$ is spinning in the same rotational direction as the rotor does and can by that

propagate with less scatter than mode $m = -1$. The transition of this mode is highly reduced in comparison with the results in Figure 8.

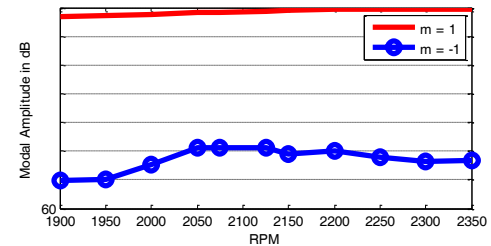


Figure 12: Modal amplitudes of spinning cut-on modes in relation to rotary speed

With increasing rotor speed the amplitude of the propagation is growing. Both modes have a slightly ascending gradient. For other frequencies this increase is nearly negligible.

4 Conclusion

While the revolution of rotor generates no further mode coupling, huge effects on the modal transition function for spinning modes are observed. By implication these have to be modeled properly for further ANC applications. Since the structure of modal transmission matrix is comparable with that of stationary rotor, the impact of spinning rotor and flow can be taken into account by factorize these according to the direction of the spinning mode. For modes rotating with the rotor the transfer function will get scaled up and vice versa while the driving speed of the fan will be ignored.

References

- [1] J. M. Tyler, T. G. Sofrin, "Axial flow compressor noise studies", *SAE Transactions*, Vol. 70, pp 309-332 (1962)
- [2] P. A. Nelson, S. J. Elliot, *Active Control of Sound*, Academic Press, London (1992)